# Dynamical Measurement of Loudspeaker Suspension Parts

Wolfgang Klippel

Klippel GmbH, Dresden, 01277, Germany

klippel@klippel.de

## ABSTRACT

The nonlinear stiffness $K(x)$ and the reciprocal compliance $C(x)$ of suspension parts (spider, surrounds, cones) and passive radiators (drones) are measured versus displacement x over the full range of operation. A dynamic, nondestructive technique is developed which excites the suspension parts pneumatically under similar condition as operated in the loudspeaker. The nonlinear parameters are estimated from the measured displacement and sound pressure signal. This guarantees highest precision of the results as well as simple handling and short measurement time.

The paper develops the theoretical basis for the new technique but also discusses the practical handling, interpretation of the results and their reproducibility.

## 1    INTRODUCTION

Transducers such as loudspeakers, headphones, shakers have a suspension realized by using a surround, spider or the diaphragm itself to center and adjust the coil in the gap and to allow a desired displacement of the moving armature. The suspension behaves like a mechanical spring characterized by a relationship between restoring force $F_k$ and instantaneous displacement $x$. Only in an ideal suspension we have a linear relationship between force and displacement and may characterize the suspension by a single number which is called stiffness $K=F_k/x$ or the inverse value compliance $C=x/F_k$. Due to the geometry of the suspension and the material properties the stiffness $K$ is usually not constant but depends on the instantaneous displacement $x$, time $t$ (frequency $f$) and the ambient

conditions (temperature, humidity). The dependency of $K(x)$ on displacement $x$ is one of the dominant nonlinearities in loudspeakers generating substantial distortion for any excitation signal below resonance.

The EIA standard RS 438 [1] describes a method for measuring the stiffness of a spider at a single displacement created by hanging a known mass from a cap at the inner diameter of the spider as illustrated in Fig. 1. While this method serves a purpose in providing a quickly-obtained estimation of spider stiffness using relatively inexpensive equipment, the measurement does not yield any information about the nonlinear behavior of the spider. Furthermore, this method may be prone to measurement error due to its highly manual nature. In the meantime additional computer controlled methods have been developed that provides the stiffness $K(x)$ versus displacement by using also a static technique. Since the stiffness $K(x,t)$ of the suspension depends on displacement $x$ and time $t$ there are discrepancies between static measurement and dynamic application of suspension part:

- The stiffness $K(x)$ measured statically at peak displacement $x=\pm X_{peak}$ is usually lower than the stiffness measured at this point with an audio-like signal. The force that is required for generating a static displacement of $x=\pm X_{peak}$ decreases slowly with time (creep).

- The stiffness $K(x)$ measured statically at rest position $x \approx 0$ is usually higher than the stiffness found by dynamic techniques.

Furthermore, other practical concerns (reproducibility, practical handling, time) gave reason for the development of a new dynamical method which measures suspension parts in the small and large signal domain.

This paper reports about this work. At the beginning the basic idea and related precursors using pneumatic excitation are discussed. Then the acoustics in the test box and the vibration of the suspension part will be modeled and the theoretical basis for a new technique developed which can be applied to spiders, cones with surrounds and passive radiators. The implementation, handling and other practical concerns will be discussed in detail later. Finally the interpretation of the results and reproducibility will be addressed and conclusions for the loudspeaker design process will be presented.
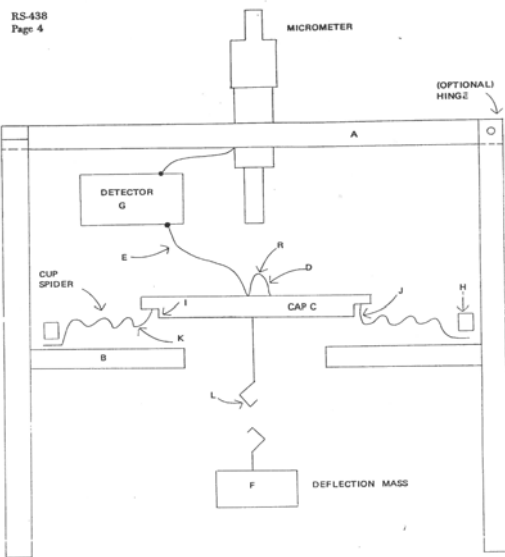
Fig. 1: Static measurement of spiders according to standard RS 438B (1976)

## 1.1 Glossary

$C(x)$      compliance of the suspension part $C(x)=1/K(x)$

$C_e$      cost function (squared error)

$C_{eff}(X_{peak})$ effective compliance depending on peak displacement $X_{peak}$

$C_{AB}$      acoustical compliance representing the enclosed air in the test box

$D_i$      inner diameter of the suspension part

$D_o$      outer diameter of the suspension part (without rim)

$D_C$      smallest diameter of the clamping cone

$e$      error signal

$E_i$      complex amplitude of the dc, fundamental and harmonic components of the error signal ($i=0,1,...$ )

$F$      total driving force at the inner clamping part

$F_K$      restoring force of the suspension

3

$F_i$        complex amplitude of the dc, fundamental and harmonic components of the restoring force ($i=0,1,...$

            )

$F_D(x)$    force representing source of nonlinear distortion generated by suspension part

$H_x(j\omega)$   linear transfer function between sound pressure $p$ and displacement $x$

$H_1(j\omega)$   ratio of the complex amplitudes of the fundamental displacement and pressure

$H_F(j\omega)$   linear transfer function between displacement x and total force $F$

$K(x)$       mechanical stiffness of suspension part

$j$          complex operator $j = \sqrt{-1}$

$k_i$        coefficients of the power series expansion of $K(x)$ with $i=0,1,...$

$K_{eff}$    effective stiffness of the suspension depending on the amplitude $X_0$, $X_1$, … of the displacement

$m$          moving mass of suspension part and inner clamping part

$m_s$        mass of suspension part

$m_c$        mass of inner clamping part

$M_{MS}$     total moving mass of a loudspeaker

$N$          maximal order of power series expansion of $K(x)$

$p(t)$       sound pressure in the test box

$P_i$        complex amplitudes of the dc, fundamental and harmonic components of the sound pressure signal

            ($i=0,1,...$ )

$p_D$        pressure ($p_D=p_e+p_{dist}$) representing the external excitation signal $p_e$ and the sound pressure distortion

            $p_{dis}$ generated by the loudspeaker

$p_0$        static air pressure

$p_{dis}$    equivalent sound pressure representing the distortion generated by the loudspeaker

$p_e$        equivalent sound pressure representing the external excitation signal

$Q_{MS}$     loss factor considering all non-electrical losses

$Q_{TS}$     Total loss factor considering all electrical, mechanical and acoustical losses in a loudspeaker

$q_D$          volume velocity generated by the loudspeaker

$q_B$          volume velocity flowing into the enclosure

$q_L$          volume velocity representing the air leakage caused by the box and porosity of the suspension

$q_S$          volume velocity due to the displacement of the suspension ($q_s = x * S_S$)

$R_{MS}$       mechanical resistance representing losses in suspension part and clamping

$R_{AL}$       acoustical resistance due to air leakage in measurement box and porosity in suspension part

$S_D$          effective area of the loudspeaker cone

$S_s$          effective area of the suspension part giving the driving force $F = S_s p$ for an air pressure $p$

$S_{geo}$      projected area of the suspension part (without clamping area)

$t$            time

$T$            time interval where the parameter identification is made

$x(t)$         displacement of the inner clamping part connected to the neck of the suspension part

$X_i$          complex amplitudes of the dc, fundamental and harmonic components of displacement ($i=0,1,\dots$ )

$\omega$       angular frequency $\omega = 2\pi f$

$\omega_0$     resonance frequency in the small signal domain where $K(x) = k_0$

$\omega_R$     effective resonance frequency in the large signal domain depending on the amplitude of the signal

$Z_D$          acoustical impedance representing the electrical and mechanical properties of the loudspeaker


## 2    BACKGROUND

The main idea is relatively simple and not new. Some loudspeaker manufacturer use for years a pneumatic excitation for suspension parts and measure the resonance frequency of the vibrating suspension. Usually a powerful loudspeaker is used for generating a sound pressure signal. In the AES standard [2] the loudspeaker cone is excited in the near field of the loudspeaker which is operated in a small panel as shown in Fig. 2. For the measurement of

spiders the loudspeaker has to be placed in a sealed test enclosure to produce sufficient sound pressure. The outer

rim  (shoulder) of the suspension part (cones or spider) is usually firmly secured by clamping rings.
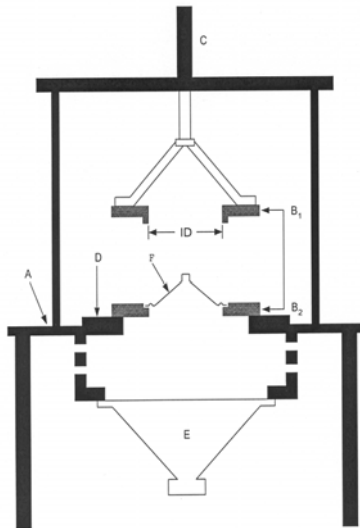


Fig.  2: Dynamic measurement of the lowest resonance frequency of  loudspeaker cones (F) according to standard AES19 (1992) using rings ($B_1$ and $B_2$) for clamping the cone rim and an additional loudspeaker (E) for acoustical excitation

Contrary to the known methods this paper suggests that the inner rim (neck) of the suspension is also clamped on a moving slide. This increases the moving mass $m$ significantly. The stiffness $K(x)$ and the moving mass m form a resonating system. At the resonance frequency the restoring force of the suspension equals the inertia of the mass. Due to the additional mass most of inertia acts directly to the neck of the suspension. Thus the suspension is operated in a similar way as in a real loudspeaker.

The new method presented here tests suspension in vertical position to avoid any offset in the displacement due to gravity as shown in Fig.  3.  An additional guiding rod for the slide may be used to prevent eccentric deformation of the suspension part and to suppress other vibration modes.

The nonlinear vibration of the suspension is measured and the unknown stiffness parameters are estimated by system identification techniques.
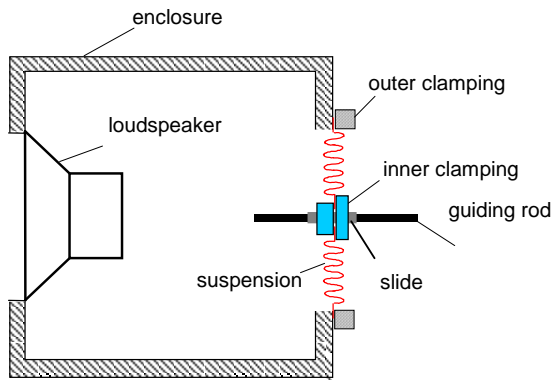


Fig. 3: Setup of the new measurement technique applied to a spider

## 3    THEORY

To understand some problems observed on existing pneumatic techniques and developing a new method for the large signal domain the physical mechanisms have to be investigated more carefully.
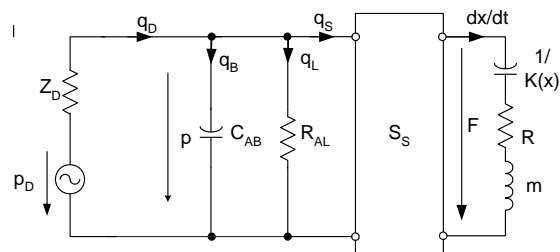


Fig. 4: Equivalent circuit of the measurement setup

### 3.1    Acoustical Modeling

Considering the setup in Fig. 3 at low frequencies where the wavelength is large in comparison to the geometry of the box the system may be modeled by the lumped parameter model shown in Fig. 4. The loudspeaker generates a volume velocity $q_D$

$$q_D = q_B + q_L + q_S \qquad\qquad (1)$$

where the volume velocity $q_B$ flows into the volume of the box, $q_L$ is leaving the box through leaks and the volume velocity $q_S$ produces the force $F$ driving the suspension part under test. To get a maximal excitation of the suspension part it would be good to keep the leakage of the enclosed air minimal. A loudspeaker with rubber surround and aluminum cone gives a good sealing. A minor leakage between the clamping parts, slide and guiding rod can not be avoided but the majority of the leakage is caused by porosity of the suspension part under test. The air in the capillaries react not as a moving mass but more like a turbulent loss represented by the resistance $R_{AL}$. It is very difficult to quantify the value of $R_{AL}$.

The pressure $p$ in the box generates a force $F=S_S p$ on the suspension part using an effective area $S_S$. In case of spiders the effective area $S_S$ has to be considered as a coupling factor between the acoustical and mechanical domain but this value is not identical with the geometrical area $S_{geo}$ and very difficult to measure. The porosity of the impregnated fabric may cause significant differences between the two areas ($S_s < 0.5\ S_{geo}$).

The acoustical compliance $C_{AB}$ depends on the volume $V$ of the enclosed air and the static air pressure $p_o$. However, the air volume is not constant but depends also on the shape of the suspension part. For example a large cone may change the effective air volume by 5 % and more.

The loudspeaker used for pneumatic excitation is modeled by an acoustical impedance $Z_D$ and a pressure source $p_D$. The pressure source comprises a sound pressure component $p_e$ generated by the electrical input of the loudspeaker and an equivalent pressure $p_{dis}$ which represents the distortion generated by the loudspeaker. However, using a loudspeaker with an extremely linear design (long coil, symmetrical suspension) the distortion $p_{dis}$ are relatively small.

The clamped suspension is described by the displacement $x$ of the inner clamping part and the driving force $F=S_s p$ which is related to the sound pressure $p$ in the test box. The driving force

$$F = pS_S = K(x) \cdot x + R_{MS}(x,v)\frac{dx}{dt} + m\frac{d^2x}{dt^2} \qquad (2)$$

is the sum of the restoring force $K(x)x$ of the suspension, the force $R_{MS}\, dx/dt$ overcoming the friction of the guiding elements and the losses in the suspension material and the inertia accelerating the mass $m$.

Not only the stiffness $K(x)$ depends on the instantaneous displacement but also the resistance $R_{MS}(x,v)$ depends on the velocity and displacement. At small amplitudes adhesive friction of the slide on the rod may cause a large nonlinearity.

The moving mass $m$ can be approximated by the total mass of suspension and the inner clamping parts

$$m \approx m_s + m_c\,. \qquad (3)$$

This approximation neglects the outer rim of the suspension which is firmly clamped during the measurement and does not contribute to the moving mass. However, the mass $m_c$ dominates the total mass $m$ and the error is in the order of 1 %. For the same reason the moving air can be neglected. The moving mass m can easily be determined by weighting the suspension with inner clamping part.

## 3.2    Measurement of State Variables

The identification of the parameter $K(x)$ requires measurement of some state variables such as force, displacement or pressure in the system.

The measurement of the displacement $x$ may be accomplished by a relatively inexpensive Laser sensor based on the triangulation principle. Careful calibration allows to measure the displacement with an accuracy of  about 1 %.

A direct measurement of the total driving force F is difficult because an integration over the $S_s$ is required. The sound pressure $p$ inside the box can easily be measured but the product $F=S_s p$ can not be calculated because the effective area $S_s$ of the suspension is usually not known.

The restoring force $F_K=K(x)x$ may be measured at the neck of the suspension at dc or at very low frequencies by using a simple force sensor. However, at higher frequencies also inertia and internal losses of the suspension part contribute to the force at the neck.

### 3.3    Small Signal Behavior

A sinusoidal sound pressure signal

$$p(t) = P_1(j\omega)e^{j\omega t} \tag{4}$$

produces a sinusoidal displacement

$$x(t) = X_1(j\omega)e^{j\omega t} \tag{5}$$

as long as the amplitude of the displacement is sufficiently small ( $X_1 \approx 0$ ) to ensure that the stiffness $K(x) = k_o$ and resistance $R_{MS}$ are constant and the system behaves linearly. The transfer function between sound pressure and displacement

$$H_x(j\omega) = \frac{X_1(j\omega)}{P_1(j\omega)} = \frac{S_s}{k_0 + j\omega\,R - \omega^2 m} \tag{6}$$

has a low-pass characteristic as shown as a thick line in Fig. 5.
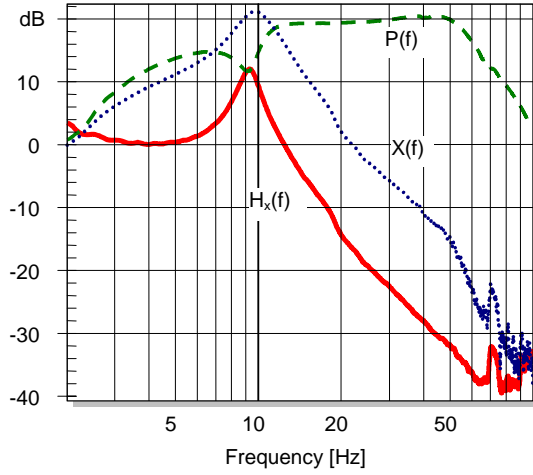
Fig. 5: Magnitude response of the sound pressure $P(f)$ (dashed line), displacement $X(f)$ (dotted line) and the transfer function $H_x(f)=X(f)/P(f)$ (thick solid line) of a 6 inch cone.

At the resonance frequency $\omega=\omega_o$ with

$$\omega_0 = \sqrt{\frac{k_0}{m}} \tag{7}$$

the restoring force of the suspension equals the inertia expressed by

$$k_o x(t) + m \cdot \frac{d^2 x}{dt^2} = 0 \, . \tag{8}$$

Since the losses of the suspension part and the friction of the clamping parts sliding on the rod are usually small, the transfer function $H_x(j\omega)$ has a distinct maximum at resonance as depicted in Fig. 5.

The size of the peak corresponds with the loss factor

$$Q_{MS} = \frac{\omega_0 m}{R_{MS}} = \frac{|H_x(j\omega_0)|}{|H_x(0)|} \tag{9}$$

which is usually high ($Q_{MS} > 2$) and describes the ratio of the magnitude of $H_x(j\omega)$ at resonance and at very low frequencies.

11

The shape of the transfer function $H_x(j\omega)$ is very similar for all kinds of suspension parts. For example, Fig. 5 – 7 show the magnitude response $|H_x(f)|$ for a 6 inch cone (with surround), a large 18 inch cone (with surround) and a 4 inch spider, respectively. However, the magnitude responses of the sound pressure $|P(f)|$ and displacement $|X(f)|$ differ significantly in all three cases. For the medium sized cone in Fig. 5 the displacement response (dotted curve) has a maximum and the sound pressure response (dashed curve) has a distinct minimum at the resonance. In this case the total acoustical impedance of the mechanical resonator (comprising $K(x)$, $R_{MS}$ and $m$) is in the same order of magnitude as the impedance of the acoustical elements (comprising $C_{AB}$ and $R_L$). Since both impedances are connected in parallel the total volume velocity $q_D$ generated by the loudspeaker splits into two parts having almost the same size at resonance where $q_S$ flows into the mechanical resonator and the $q_B+q_L$ into the box and leaks.
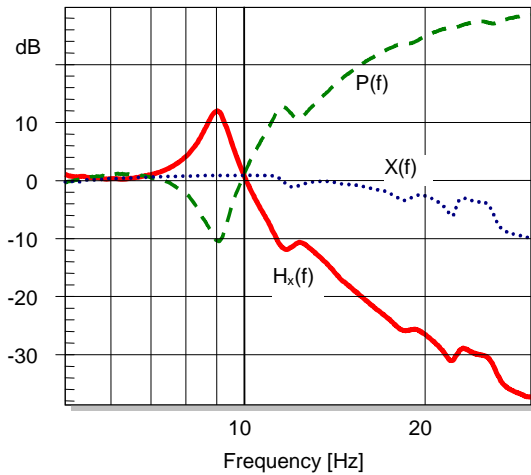


Fig. 6: Magnitude response of the sound pressure $P(f)$ (dashed line), displacement $X(f)$ (dotted line) and the transfer function $H_x(f)=X(f)/P(f)$ (thick solid line) of a 18 inch cone.

For a larger diameter of the suspension the acoustical impedance of the mechanical resonator becomes smaller with $1/S_S^2$. Thus, for the 18 inch cone the acoustical impedance of the resonator at resonance is much smaller than the impedance of the acoustical elements and almost the complete volume velocity of the loudspeaker flows into the mechanical resonator ($q_D \approx q_S$). The acoustical impedance of the mechanical resonator becomes also much lower than the acoustical impedance $|Z_D|$ of the loudspeaker. Thus the volume velocity $q_D$ is almost independent of the mechanical resonator and the displacement response $|X(f)|$ depicted as dotted line in Fig. 6 has no resonance peak.

Only the sound pressure response $|P(f)|$ depicted as dashed line has a distinct minimum at resonance revealing the effect of the resonator.
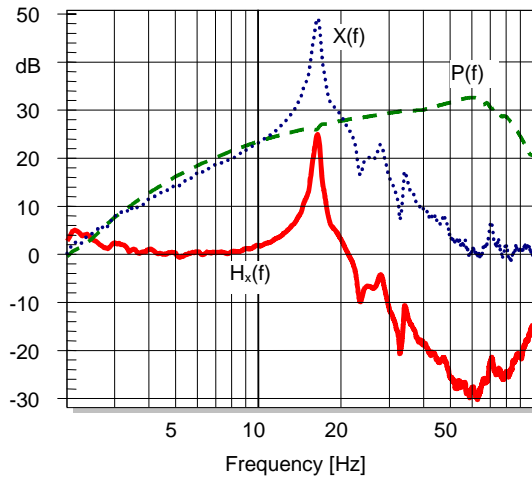


Fig. 7: Magnitude response of the sound pressure $P(f)$ (dashed line), displacement $X(f)$ (dotted line) and the transfer function $H_x(f)=X(f)/P(f)$ (thick solid line) of a 4 inch spider.

Suspension parts with a small effective area $S_S$ such as the 4 inch spider lead to the opposite case. Here the acoustical impedance of the mechanical resonator is relatively high (due to the transformation into acoustical elements with $1/S_S^2$) and the acoustical compliance $C_{AB}$ and the resistance $R_L$ is much lower. This keeps the sound pressure response $|P(f)|$ shown as dashed line in Fig. 7 constant at resonance. Only the displacement response $|X(f)|$ depicted as dotted line reveals the effect of the mechanical resonator.

These examples show that the detection of the resonance for any kind of suspension part can not be accomplished by performing a single acoustical measurement of sound pressure p or a single mechanical measurement of displacement x but requires in general a combination of both measurements and the calculation of the transfer response $H_x(j\omega)$.
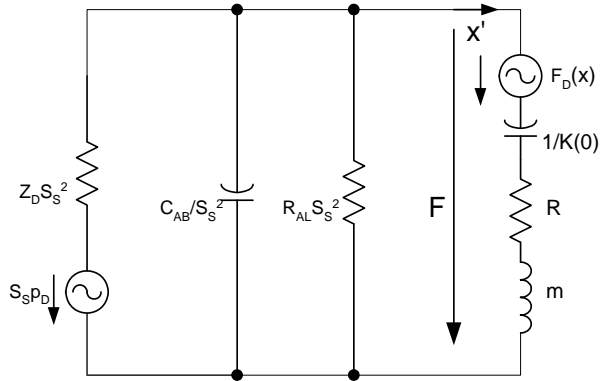
Fig. 8: Generation and propagation of harmonic distortion in the test set up

## 3.4    Large Signal Behavior

At higher amplitudes the varying stiffness *K(x)* generates a nonlinear vibration behavior of the suspension. For a sinusoidal excitation voltage the sound pressure signal in the enclosure is

$$p(t) = P_1 e^{j\omega t} + P_2 e^{j2\omega t} + P_3 e^{j3\omega t} + ... \tag{10}$$

and displacement of the inner rim of the suspension part

$$x(t) = X_0 + X_1 e^{j\omega t} + X_2 e^{j2\omega t} + X_3 e^{j3\omega t} + ... \tag{11}$$

comprises a dc component $X_0$, a fundamental component $X_1$, and   $P_1$ and harmonics $X_i$ and $P_i$, respectively, at frequencies $i\omega$ with the order $i > 1$.

To make this complicated mechanism more transparent the restoring force $F_K(t)$ is spitted into a   linear and a nonlinear part

$$F_K = K(0)x + F_D(x) = K(0)x + \left(K(x) - K(0)\right)x \bullet \tag{12}$$

14

The linear term in Equation (12) uses the constant stiffness $K(0)$ while the nonlinear term represents the variations of the stiffness only. This term may be considered as a new source supplying distortion $F_D(x)$ into the equivalent circuit shown in Fig. 8.
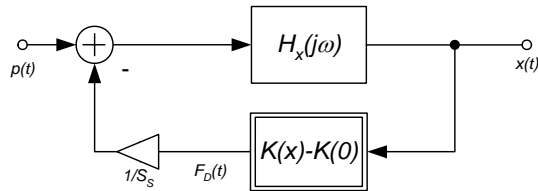


Fig. 9: Large signal model of the suspension part

Inserting Equation (12) into Equation (2) The transfer of the $F_D$ to the displacement $x$ can be modeled by the signal flow chart depicted in Fig. 9. The varying part $K(x)-K(0)$ of the stiffness represented as a static nonlinearity (without any memory) generates the distortion force $F_D$ which is transformed into a sound pressure component by the effective area $S_S$ of the suspension and subtracted from the pressure in the test enclosure. The total pressure is transformed via the linear transfer function $H_x(j\omega)$ in Equation (6) into the displacement signal $x(t)$.

The nonlinear force $F_D$ generates not only a dc component and harmonics but also a component at the fundamental frequency $\omega$. This fundamental distortion component has a significant effect on the behavior of the system at resonance because the feed-back loop in Fig. 9 has a high gain due to the loss factor ($Q_{MS} > 2$) of $H_x(j\omega)$.
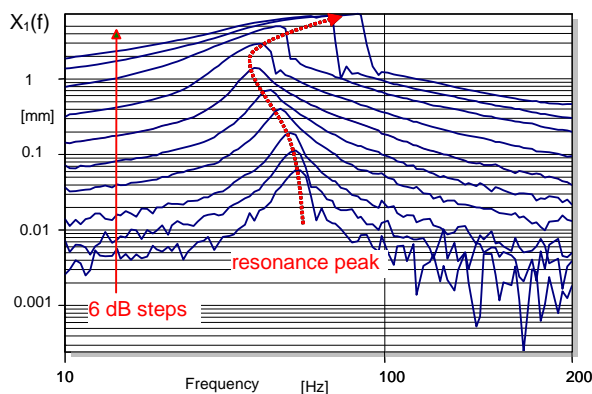


Fig. 10: Amplitude response of the displacement while increasing the excitation amplitude by 6 dB

For example, Fig. 10 shows the amplitude response of the fundamental displacement component $X_1$ where the excitation amplitude is increased by 6 dB increments. At small amplitudes the curve has an almost symmetrical resonance peak but becomes more and more asymmetrical at higher amplitudes. The resonance peak is also shifted to higher frequencies at large amplitudes.

For sinusoidal excitation the complex ratio $H_1(j\omega)$ of the fundamentals $X_1$ and $P_1$ in the displacement and sound pressure spectrum, respectively, may be expressed as

$$H_1(j\omega) = \frac{X_1(j\omega)}{P_1(j\omega)} = \frac{S_s}{K_{eff}(X_{peak}) + j\omega\,R - \omega^2 m} \tag{13}$$

using the effective stiffness $K_{eff}$ which depends on the stiffness characteristic $K(x)$ and the peak displacement $X_{peak}$.

At a particular frequency

$$\omega_R(X_{peak}) = \sqrt{\frac{K_{eff}(X_{peak})}{m}} \tag{14}$$

the real part

$$K_{eff}(X_{peak}) - \omega_R{}^2 m = 0 \tag{15}$$

in Equation (13) vanishes and $|H_1(j\omega)|$ becomes maximal if the mechanical losses represented by resistance $R_{MS}$ are sufficiently small.

The frequency $\omega_R$ may be understood as a *large signal resonance frequency* depending on the peak displacement $X_{peak}$ in contrast to the (small signal) resonance frequency which is a constant value $\omega_0$ in the linear model. Due to the low losses in the suspension and the high loss factor ($Q_{MS} > 2$) the large signal resonance frequency may also be detected by searching for the maximum in $|H_1(j\omega)|$.

However, driving the system into resonance is not so trivial at high amplitudes as in the small signal domain. Since the effective stiffness usually increases with peak displacement $X_{peak}$ the large signal resonance frequency $\omega_R$ is usually much higher than the small signal resonance $\omega_0$. Performing a sinusoidal sweep with falling frequency leads

to a maximum at much smaller frequencies than sweeping with rising frequency. The reason for this phenomenon is illustrated in Fig. 11. Due to the displacement depending resonance $\omega_R(X_{peak})$ and the high $Q_{MS}$ there is a bifurcation into three states on the right side of the backbone curve whereas only two states are stable.
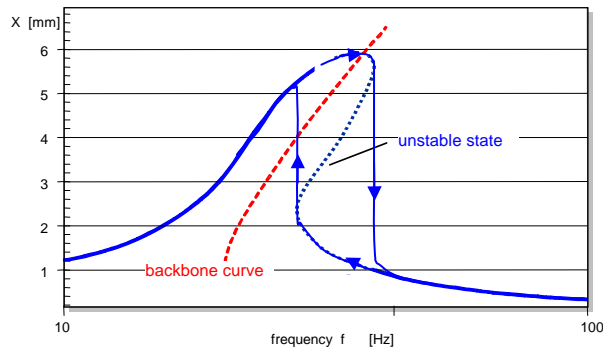


Fig. 11: Amplitude response of displacement at high amplitudes measured with a sinusoidal sweep with rising and falling frequency.

Performing a sweep with rising frequency started one third-octave below the large signal resonance usually leads the nonlinear resonator into the upper state and the large signal resonance $\omega_R(X_{peak})$ can be found where the ratio $|H_1(j\omega)|$ between the fundamentals becomes maximal. Performing a sweep with falling frequencies the system usually uses the path via the lower states and the system actually misses the large signal resonance. A similar result may be obtained by exciting the suspension with a fixed frequency at $\omega_R$ by increasing the excitation amplitude slowly. The resonator remains in the lower state and finally at very high excitation or by any perturbation (a manual kick giving to the suspension) the resonator jumps into the upper state which is usually below resonance.

### 3.5     Identification of the Parameters

With the knowledge about the physics of the acoustical system a dynamical measurement technique will be developed here.

As said before the main idea is to realize with an appropriate inner clamping of the suspension part a clear defined moving mass and to operate the suspension in the resonance. Since the losses in the suspension are small and the $Q$-factor is usually high the resonance can easily be detected by searching for a distinct maximum in the ratio $|H_1(j\omega)|$.

Operating the suspension part in the resonance has also the benefit that a small box pressure generated by the loudspeaker gives maximal displacement of the suspension.

The next point is that the suspension is excited by a sweep signal starting at least one-third octave below resonance ending approximately one-third octave above resonance. The displacement of the inner clamping parts and the sound pressure in the box is measured by sensors (laser triangulation sensor and microphone inside the box) and provided as time signals to the signal processing. For the measurement of spiders and smaller sized cones the sound pressure measurement may be omitted as discussed in detail below.
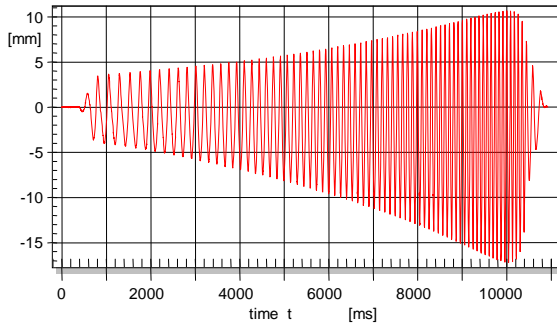


Fig. 12: Voice coil displacement of an asymmetric suspension (spider) while sweeping over the resonance frequency

For example, Fig. 12 shows the recorded displacement signal where the characteristic decay of the amplitude above resonance is clearly visible.

Searching for a maximum in the displacement pressure ratio $|H_1(j\omega)|$ leads to the effective resonance frequency $\omega_R$ if the loss factor $Q_{MS}$ is greater than 2. The loss factor should always be checked to get an indication for bad clamping of the suspension and possible excessive friction at the slide on the guiding rod.

### 3.5.1 Effective Stiffness $K_{eff}$

Knowing the effective resonance frequency $\omega_R$ and the moving mass $m$ the effective stiffness

$$K_{eff}(X_{peak}) = \omega_R{}^2 m \tag{16}$$

or

the effective compliance

$$C_{eff}(X_{peak}) = \frac{1}{\omega_R^2 m}$$ (17)

are calculated. Since the resonance frequency $\omega_R$ depends on the amplitude of the displacement, the effective stiffness should also be understood as a function of the displacement $X_{peak}$.

The measurement of the effective stiffness can be accomplished with straightforward measurement equipment.

### 3.5.2    Nonlinear Stiffness *K(x)*

More detailed information about the properties of the suspension give the displacement varying stiffness *K(x)*. The curve can be calculated from the harmonic distortion found in the sound pressure and displacement  signal. For example Fig.  13 shows the spectrum of one period of the displacement time signal located at the maximum in Fig. 12.
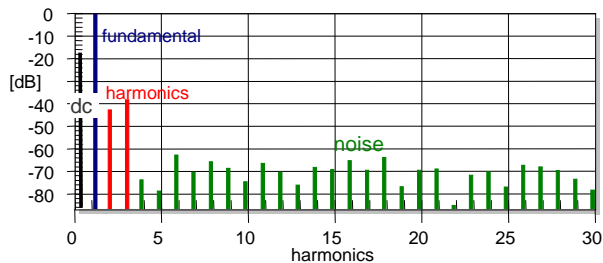


Fig. 13: Spectrum of one period of the displacement at resonance frequency $\omega_R=15\ Hz$  generated by sinusoidal excitation

The spectrum in Fig. 13 comprises a fundamental, a dc component, a 2nd-order and 3rd-order components which are clearly above the noise floor. The dc-component is generated dynamically by the asymmetry of the stiffness and depends also on the amplitude. The dc component is also visible in Fig.  12. At the beginning of the measurement

the displacement is almost symmetrical but becomes asymmetrical at higher amplitudes. The bottom value (-17 mm) is at resonance $\omega_R$ much lower than the peak value (+11 mm) which gives the raise of the even-order harmonics.

The balance of the forces in the mechanical resonator expressed in equation (2) is the basis for the identification of the nonlinear stiffness. Considering measured displacement and sound pressure signals corrupted by noise and calibration errors the ideal Equation (2) is written as the model error equation

$$e = K(x) \cdot x + R_{MS}\frac{dx}{dt} + m\frac{d^2x}{dt^2} - S_S p \,. \tag{18}$$

The shape of the nonlinear $K(x)$ characteristic is estimated by straightforward optimization where the squared error in the cost function

$$C_e = \frac{1}{T}\int_0^T e(t)^2\,dt \quad \rightarrow \quad Minimum \tag{19}$$

is minimized over a certain time interval $T$. To search between a wide variety of candidates for the curve shape, $K(x)$ is expressed by a truncated power series expansion

$$K(x) = \sum_{i=0}^{N} k_i x^i \,. \tag{20}$$

Since there is a linear relationship between the unknown coefficients $k_i$ $(i=0,1,\ ...\ N)$ and the error signal $e(t)$ the coefficients can be estimated by searching for the minimum in the cost function in a $(N+1)$-dimensional space by solving a linear set of equations

$$\frac{\partial C_e}{\partial k_i} = 0 \,. \tag{21}$$

The error equation (18) still requires precise values for the additional parameters moving mass $m$, mechanical resistance $R_{MS}$ and effective area $S_s$. While the moving mass $m$ can easily be measured by weighting the suspension part with inner clamping, the resistance $R_{MS}$ and effective area $S_S$ can not be measured directly.

This problem can be solved by using a modified error equation (25) developed as a *Two Signal Method* in the appendix. The driving force *F* is not described by the unknown effective area $S_S$ but is estimated by the measured transfer function $H_x(j\omega)$ between sound pressure *p* in the test box and the displacement signal *x*. Here values of $H_x(j\omega)$ at frequencies above the large signal resonance $\omega_R$ are required. This measurement can be easily performed by a first pre-measurement using a wide-band sweep. The amplitude of the stimulus is not critical because $H_x(j\omega) \approx H_1(j\omega)$ for $\omega > \omega_R$.

This technique puts minimal requirements on the microphone used and still works if the microphone is not calibrated and has a poor amplitude response. Also the position of the microphone inside the box and any time delay in the measurement path is not critical as long as the same position is used in the pre- and main-measurement. However, the microphone should behave linearly at the sound pressure amplitudes occurring in the test enclosure. The laser displacement sensor should be calibrated carefully.

For spiders and smaller sized cones the sound pressure measurement can be omitted and the simple *One Signal Method* developed in the appendix may be used. If the acoustical compliance of the test box is large in comparison to the compliance of the suspension part, then a simplified error equation (38) developed in the appendix can be used. A simple but reliable criteria for the validity of this method is the distinctness of the resonance peak found in the displacement frequency response $|X(f)|$. For example the displacement response $|X(f)|$ of the 6 inch cone in Fig. 5 and the 4 inch spider in Fig. 7 show a distinct maximum in the displacement. However, the resonance of the large 18" cone leads to a sound pressure minimum and is almost not detectable in the displacement signal. Suspension parts with a large area $S_s$ should always be measured by using the *Two Signal Method*.

### 3.5.3    Resistance $R_{MS}$

In the small signal domain the suspension with inner clamping may be measured without using a guiding rod. According to Equation (9) the resistance

$$R_{MS} = \frac{\omega_0 m}{Q_{MS}} = \omega_0 m \frac{|H_x(0)|}{|H_x(j\omega_0)|}  \tag{22}$$

may be calculated by using the known mass $m$, the resonance frequency $\omega_o$ and the measured transfer function $H_x(j\omega)$. Measurements at high amplitudes require some guidance of the inner clamping part and the friction contributes to the measured resistance $R_{MS}$ and the losses of the suspension can not be measured separately. However, the suspension losses have only a small impact on the final loudspeaker performance for two reasons:

- The flow resistance of the air passing the voice coil in the gap contributes significantly to the total mechanical $Q_{MS}$.

- In a voltage driven loudspeaker system the electrical damping dominates the total loss factor $Q_{TS}$ .

## 4    PRACTICAL USAGE

After developing the theoretical basis of the dynamic measurement technique the implementation and practical handling is shortly addressed.

### 4.1    Hardware Requirements

The following hardware components are required to realize the One Signal Method:

#### 4.1.1    Measurement box with excitation loudspeaker

The box should be as large as possible to make the compliance $C_{AS}/S_D^2$ large and to provide a constant excitation force for the mechanical resonator in Equation (2). The loudspeaker used for pneumatic excitation should be an 18 inch woofer with sufficient $X_{max}$ providing sufficient air flow.

#### 4.1.2    Inner Clamping Tool

The suspension part should be clamped during the dynamic testing in a similar way as mounted in the final loudspeaker.

If destructive testing is applicable the suspension part can be glued to original loudspeaker parts (voice coil former, frame) which can more easily be mounted in the measurement box.

A nondestructive testing is preferred for comparing samples, storing reference units and for simplifying the communication between manufacturer and customer.

Since most of the suspension parts have an axial-symmetrical shape they can be clamped by a universal clamping set comprising a minimal number of clamping parts (cups and cones).

If the nonlinear stiffness of the suspension part shall be measured in the large signal domain additional guidance of the inner clamping part is required. This can be realized by using a sleeve sliding at low friction on a high polished center rod. The suspension has to be clamped on the slide in such a way that the outer rim of the suspension is in the middle of the slide. For a very asymmetric suspension parts such as a loudspeaker cone an additional mass may be added on the other side to ensure that the center of gravity is also in the middle of the slide as illustrated in Fig. 14. This reduces tilting of the suspension, irregular vibration and ensures minimal friction at the rod.
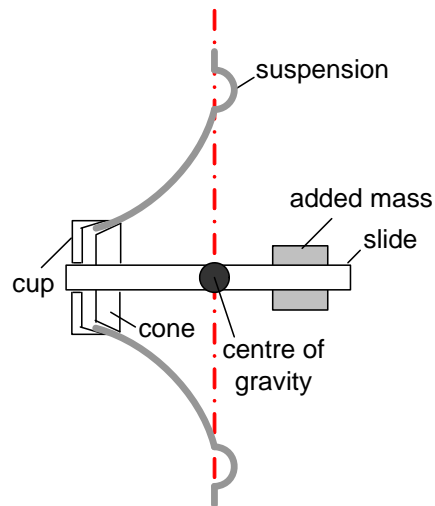


Fig. 14: Optimal inner clamping of a suspension having an asymmetrical geometry (loudspeaker cone)

### 4.1.3    Scale

Finally the weight of the suspension with inner clamping parts is measured and provided to the post processing software.
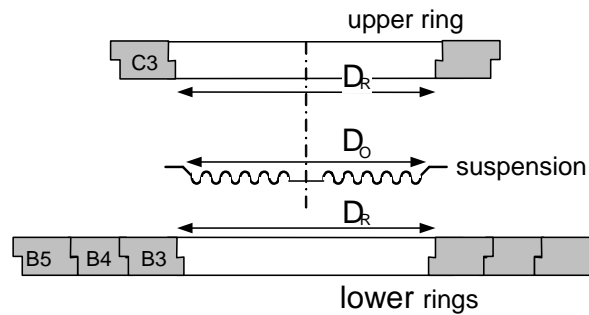


Fig. 15: Outer clamping of the suspension using a universal ring set

### 4.1.4    Outer Clamping Tools

The outer clamping of axial-symmetrical suspension parts can be realized by using a set of rings as illustrated in Fig. 15. Knowing the outer dimension $D_O$ of the suspension the lower ring (for example **B3**) is selected from a look up table. As illustrated in Fig. 15 the outer diameter $D_O$ should be just smaller than the ring diameter $D_R$. The free space in the opening of the measurement box is closed by other rings which have the same character in the nomenclature (**B**) and are larger than the lower clamping ring (**B4**, **B5, B6**). Finally the next larger ring (**C3**) is used as upper clamping ring because it provides a rim with the same diameter $D_R$ on the opposite side.

### 4.1.5    Laser Displacement Sensor

A laser sensor is used to measure the displacement of the inner clamping part.

### 4.2    Performing the measurement

The measurement is performed in two steps:

### 4.2.1    Pre Measurement

A first measurement performs a wide band sweep (from 5 Hz to 100 Hz) to measure the transfer function $H_1(j\omega)$ in the case of the *Two Signal Method* or just the amplitude response $X(j\omega)$ for the *One Signal Method* as shown in Fig. 5. This data is used to find the resonance frequency and calculates optimal setup parameter.

### 4.2.2    Main measurement

The main measurement performs a narrow band sweep starting one-third octave below the mechanical resonance and ending just after the jumping effect above the resonance. For the 4 inch spider the measured displacement $x(t)$ is shown in Fig. 12. If the peak displacement does not meet the target value specified by the user the main measurement is repeated after adjusting the voltage of the stimulus. By using an automatic voltage control a complete measurement can be accomplished in less than a few minutes.
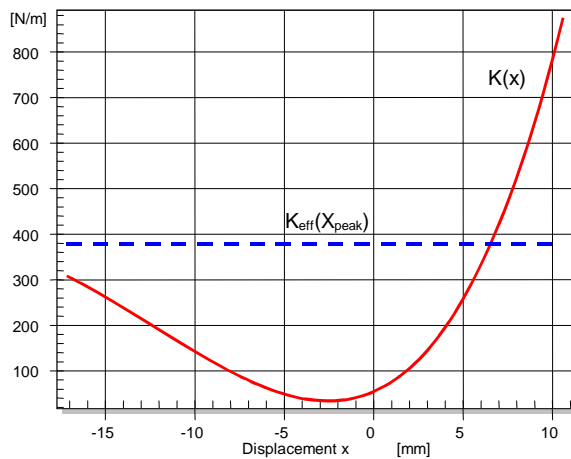


Fig. 16: Nonlinear stiffness $K(x)$ (solid line) and effective stiffness $K_{eff}$ (dashed line) of a cup spider
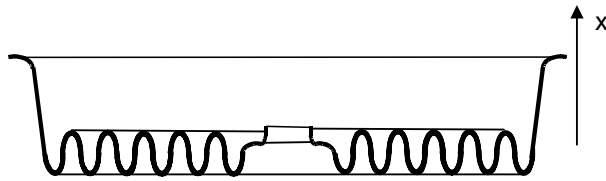
Fig. 17: Cross sectional view of a cup spider

## 5    INTERPRETATION

### 5.1    Nonlinear Stiffness K(x)

Fig. 16 shows the stiffness characteristic $K(x)$ versus voice coil displacement of a cup spider having a geometry as illustrated in Fig. 17. For a positive displacement $x=+11$ mm the stiffness value is approximately 30 times higher than at the rest position $x=0$. The stiffness characteristic has also a distinct asymmetry. At negative displacement $x=-11$ mm the stiffness is only 16 % of value found at positive displacement $x=+11$ mm. Such an asymmetrical stiffness is directly related with the typical geometry of a cup spider because the outer rolls provide less stiffness for radial force and move to the center especially for a negative deflection. However, the asymmetry of the outer rim (shoulder) can be compensated by the size, geometry of the inner corrugation role which has also an inherent asymmetry. This is also the reason why a plane spiders may show an asymmetrical stiffness if the number of corrugation rolls is low and the shape of the inner (half) roll and inner rim are not optimal.

However, any asymmetry in the K(x)-characteristic causes a partial rectification of the ac-signal and generates a dc-component always to the softer side of the suspension. The cup spider measured in Fig. 17 may produce a dynamic voice coil offset of - 3 mm.
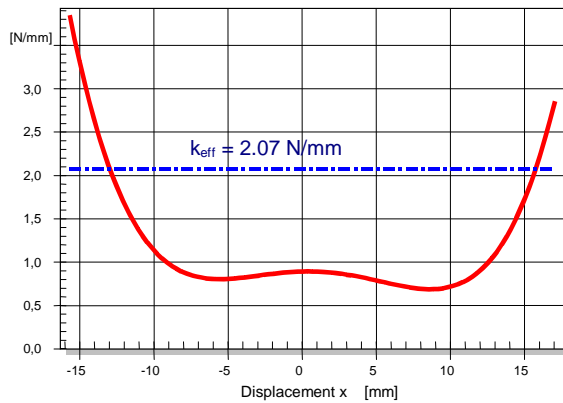
Fig. 18: Nonlinear stiffness *K(x)* (solid line) and effective stiffness $K_{eff}$ (dashed line) of a cone with surround.

Fig. 18 shows the nonlinear stiffness K(x) as a solid line of a cone with a surround having a half roll as illustrated in Fig. 14. For such kinds of suspension parts the stiffness characteristic has an almost constant plateau at low and medium displacement but rises rapidly at higher values where the displacement is not small compared with the diameter of the half roll. The asymmetrical geometry inherent in most surrounds cause also an asymmetry in the stiffness.

## 5.2    Effective Stiffness

The dashed curve in Fig. 16 shows the effective stiffness $K_{eff}$ of the suspension in the working range (-17< x < +11).
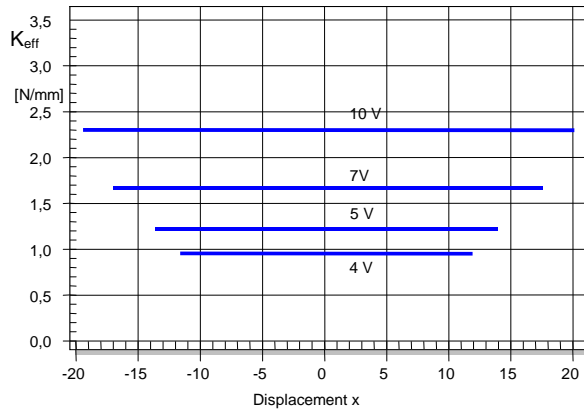
Fig. 19: Effective Stiffness $K_{eff}(X_{peak})$ depending on the amplitude of displacement

The effective stiffness $K_{eff}(X_{peak})$ depends on the maximal peak displacement $X_{peak}$ occurred during measurement. Fig. 19 shows the variation of the effective stiffness of a 3 inch spider measured with slowly increased voltage from 4 to 10 V at the terminals of the loudspeaker. The substantial variations at higher amplitudes are mainly caused by the nonlinear increase of the stiffness at higher displacement.

To ensure comparability of the results the peak displacement $X_{peak}$ should be stated for which the effective stiffness $K_{eff}(X_{eak})$ is valid such as

$$K_{eff}=0.4 \text{ Nmm}^{-1} \ @ \ X_{peak}=17 \text{ mm}.$$

This value is simple to interpret and corresponds directly with the resonance frequency $\omega_R$ and the moving mass $m$. It is a single-number representation of $K(x)$ which may be sufficient and convenient for QC applications.
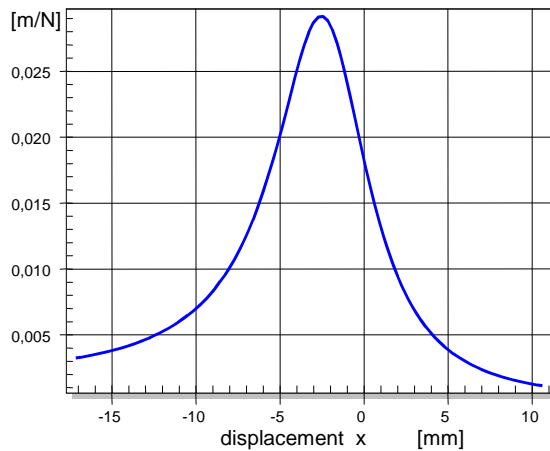
Fig. 20: Nonlinear compliance C(x) of a cup spider corresponding to the nonlinear stiffness in Fig. 16

### 5.3    Compliance *C(x)*

The compliance *C(x)* is just the inverse of the stiffness *K(x)*. For the 4 inch spider Fig. 20 shows a bell-shaped curve which corresponds with the parabola found in the *K(x)* characteristic in Fig. 16. However, the stiffness curve reveals details of the nonlinearity clearer than the compliance curve and is better suited for graphical representation.

### 6    IRREGULAR SUSPENSION BEHAVIOR

Suspension parts are usually made out of impregnated cloth, paper, foam and rubber having properties which vary with time (breaking in, creep, aging) and depend on the ambient conditions (temperature, humidity). Some of the variations are irreversible (breaking in) but other processes are reversible after a certain time constant.

The new dynamic measurement technique developed here gives new insight into those complicated mechanisms:
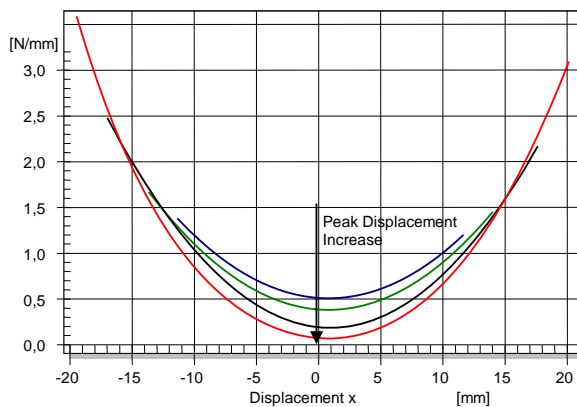
Fig. 21: Nonlinear stiffness of a plan spider as a function of the amplitude

## 6.1   Reversible Variations

Fig. 21 shows the nonlinear stiffness $K(x)$ measured with different amplitudes of the excitation signals. Whereas the curves at positive and negative peak values $X_{peak}$ almost coincide there is a significant decrease of stiffness $K(x=0)$ at the rest position $x=0$. This is not an artifact of the measurement but a typical property of the material. The same behavior has been observed in final loudspeaker using other static, quasi-static or dynamic methods [4], [5], [6]. At small signal amplitudes this effect dominants the increase of the stiffness at the positive and negative peak value. Thus the effective stiffness $K_{eff}(X_{peak})$ and resonance frequency $\omega_R(X_{peak})$ fall with rising peak displacement. This irregular behavior is also the reason in the decreasing resonance frequency in Fig. 10 for $X_{peak} < 2mm$.

A simple explanation for this phenomenon is that stretching of the corrugation rolls at high amplitudes causes a temporary deformation of the fiber structure and makes the suspension softer between the positive and negative peak values. The spider in Fig. 21 for example loses temporarily almost all the stiffness at the rest position just after performing a peak to peak displacement of 40 mm. This kind of deformation stays only for a short time constant (multiple periods of the ac signal) and recovers completely after a few seconds. This is an reversible process which depends on the geometry and impregnation of the suspension material. It increases the nonlinearity of the suspension which becomes not only stiffer for larger displacement but also softer between the excursion maxima.
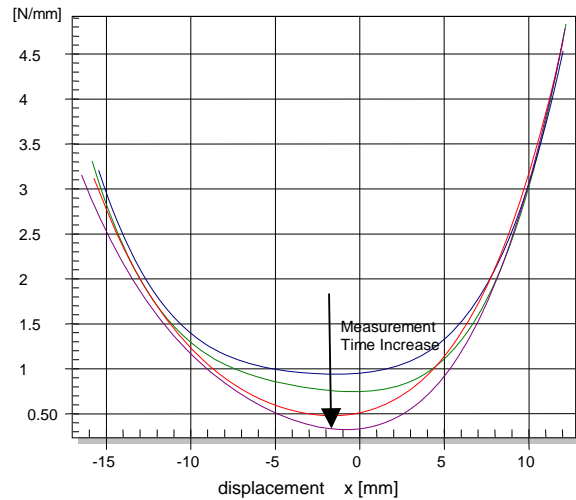
Fig. 22: Variation of the nonlinear stiffness K(x) of a cup spider during long term testing of a spider (measured in 15 min intervals)

## 6.2    Irreversible Changes

The dynamic measurement technique is also convenient for the investigation of the break in and other ageing effects of the suspension. The example in Fig. 22 shows the change of the stiffness versus measurement time. The spider under test is permanently excited with an audio-like test signal and measurements are taken after 15 min intervals. It is interesting to see that the stiffness at higher displacements stays constant but the stiffness at the rest position x=0 is reduced down to 30 %. Thus the stiffness at high positive and negative displacement is closely related with the geometry of the suspension while the stiffness at rest position is mainly determined of the impregnation and thickness of the material.

## 7    REPRODUCIBILITY

The reproducibility and repeatability of the new measurement technique has been investigated systematically. A series of test has been performed on a variety of different suspension parts to assess the influence of the following factors:

- clamping the suspension part

- additional mass of the inner clamping parts

- influence of the stimulus

- maximal order $N$ of the power series expansion used for $K(x)$

- uncontrolled variables (other nonlinearities in the measurement setup)

At first the repeatability of the measurement technique has been tested on suspension parts without changing the clamping and the setup. The results are very reproducible ( < 1%). If the measurement were repeated more than 10 times, the stiffness $x$=0 has the tendency to decrease to lower values systematically. This effect can be reduced by exposing test objects before measurement to a break-in procedure (5 min vibration at resonance).

The outer clamping has a minor influence on the measurement results. Even operating faults such as using rings which are too small or are not applied concentrically cause relatively small errors.

The inner clamping is much more critical. Some care is required to ensure that the friction of the slide on the rod is small, the displacement of the inner corrugation roles is not limited by the inner clamping parts. The center of gravity and the outer clamping plane should be approximately in the middle of the slide. If the friction is too high giving a low $Q_{MS}$ of the resonator, then the maximum of the transfer function $H_x(j\omega)$ occurs below resonance frequency giving a smaller estimate of the stiffness.
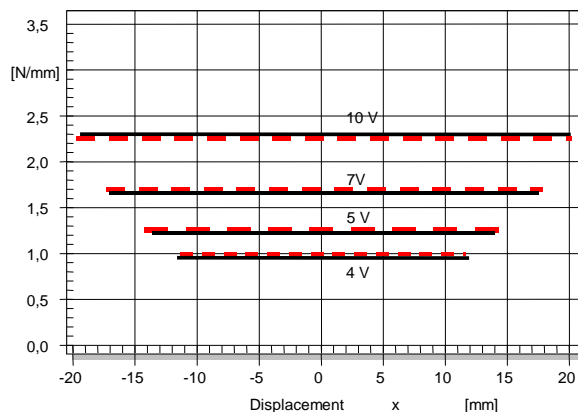
Fig. 23: Effective (mean) stiffness $K_{eff}$ measured on a spider at different amplitudes (excitation voltages 4V, 5V, 7 V and 10V) and with two different masses 297 gram (dashed line) and 327 gram (solid line).
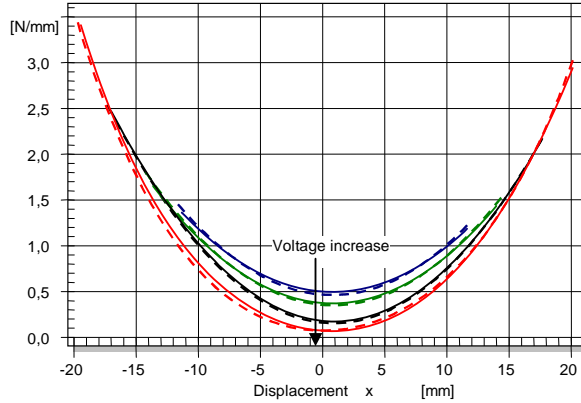


Fig. 24: Stiffness $K(x)$ versus displacement x of a spider measured with different amplitudes (excitation voltages 4V, 5V, 7 V and 10V) and with two different masses 297 gram (dashed line) and 327 gram (solid line).

The influence of the additional mass $m_c$ provided by the inner clamping parts has also been investigated. The higher the additional mass the lower the resonance frequency of the resonator. At lower frequencies time reversible processes in the suspension become more dominant and the fibers in the suspension have enough time to change their position. This reduces the effective stiffness to lower frequencies as described by Knudsen [7]. It also explains why the stiffness measured statically is usually lower than measured dynamically at higher frequencies.

Fig. 23 shows the effective stiffness $K_{eff}(X_{peak})$ measured at four amplitudes for two different masses represented as dashed and solid lines. Fig. 24 shows the influence of the mass variation in the corresponding $K(x)$ curves measured at the same amplitudes. The variations caused by amplitude variation are much higher than the influence of the moving mass.

The influence of the stimulus is small as long as the starting frequency is set at least one-third octave below the large signal resonance to ensure that the nonlinear resonator passes the upper vibrating state.

Finally the order $N$ used in the power series expansion of $K(x)$ has a large influence on the shape of the measured $K(x)$ curve. Depending on the signal to noise ratio in the displacement measurement the order $N$ has to be limited

*(N<5)*. The SPM software provides an automatic determination of the maximal order *N* according to the noise floor. To compare curves from different measurements it is recommended to use fittings of the same order *N*.

## 8    CONCLUSION

A new technique for measuring the most important mechanical properties of suspension parts (cones with surround, spiders) is presented which also reveals the nonlinear characteristic in the full working range.

The stiffness *K(x)* displayed versus displacement x is the most important parameter for suspension parts. The inverse parameter compliance *C(x)* gives no additional information but shows the nonlinear characteristic at higher amplitudes not so clearly as the *K(x)*. The effective stiffness $K_{eff}(X_{peak})$ or compliance $C_{eff}(X_{peak})$  are integral measures of the corresponding nonlinear parameters *K(x)* and *C(x)* in the used working range defined by the peak value $X_{peak}$. The effective parameters are directly related with the resonance frequency and may be measured with conventional equipment. However, the effective parameters can only be compared if the  measurement are made at the same peak displacement $X_{peak.}$

The nonlinear stiffness *K(x)* or compliance *C(x)* reveal the causes of the nonlinear signal distortion generated by the suspension. This parameter together with parameters of the motor such as force factor *Bl(x),* inductance *L(x)*) are the basis for numerical prediction of the loudspeaker behavior at high amplitudes. Thus the maximal output and the generation of harmonic and intermodulation distortion can be simulated. For example, a symmetrical increase of the stiffness *K(x)* versus positive and negative excursions generates third-order and other odd-order distortion, limits the maximal displacement. A symmetrical increases of stiffness is desirable to some extent and provides natural protection of the voice coil from hitting the back-plate. Asymmetries should always be avoided. They generate not only 2nd- and higher order distortion but also generate a dc displacement which shift the coil dynamically away from the optimal rest position and are the cause for instabilities [3].

The pneumatic excitation of the suspension part allows a dynamic measurement of the suspension part vibrating at frequencies at the lower limit of the audio band. Thus, memory effects of the suspension (frequency depending stiffness *K(f),* creep and dependency of *K(x=0)* on $X_{peak}$) occur almost in the same way as in the final loudspeaker.

The usage of an additional mass clamped to the neck of the suspension increases the precision of the calculated stiffness because the uncertainty of the moving mass $m$ can significantly reduced.

The operation of the suspension part in vertical position is not only mandatory due to the additional mass but also important for larger cones where the weight of the cone material itself causes a significant offset in displacement giving a higher stiffness value if measured in horizontal position.

The technique may not only be applied to all kinds of suspension parts but can also be used for passive radiators (drones). The moving mass $m$ is equal to $M_{ms}$ which may be estimated by the straightforward techniques (added mass method performed at low amplitudes).

Exploiting modern signal processing and identification techniques in combination with pneumatic excitation leads to a new measurement which provides not only repeatable and reproducible results but is also very fast, robust and simple to use.

## 9    REFERENCES

[1] "ANSI - Standard : Electronic Industries Association RS 438 – Loudspeaker Spiders, Test for Measuring Stiffness," Irvine, Global Engineering Documents (1976).

[2] "AES–ALMA Standard test method for audio engineering — Measurement of the lowest resonance frequency of loudspeaker cones," AES19-1992 (withdrawn 2003) (ALMA TM-100), *published by* Audio Eng. Society, (1992).

[3] W. Klippel, Tutorial: Loudspeaker Nonlinearities - Causes, Parameters, Symptoms *J. Audio Eng. Society* **54**, No. 10  pp. 907-939 (2006 Oct.).

[4] M. Knudsen, J.G. Jensen, V. Julskjaer and P. Rubak, "Determination of Loudspeaker Driver parameters Using a System Identification Technique," *J. Audio Eng. Soc.* vol. 37, No. 9.

[5] S. Hutt, "Loudspeaker Spider Linearity," presented on 108th Convention of the Audio Eng. Soc., Paris, 19-22nd February, 2000, Preprint 5159.

[6] D. Clark, „Precision Measurement of Loudspeaker Parameters," *J. Audio Eng. Soc.* vol. 45, pp. 129 - 140 (1997 March).

[7] M.H. Knudsen and J.G. Jensen, "Low-Frequency Loudspeaker Models that Include Suspension Creep*," J. Audio Eng. Soc.*, vol. 41, pp. 3-18, (Jan./Feb. 1993)

[8] W. Klippel, U. Seidel, "Fast and Accurate Measurement of Linear Transducer Parameters," presented at the 110th Convention of the Audio Engineering Society, Amsterdam, May 12-15, 2001, preprint 5308, J. Audio Eng. Society, Vol. 49, No. 6, 2001 June, P. 526.

[9] "Suspension Part Measurement (SPM)," Specification of the KLIPPEL analyzer module, Klippel GmbH, 2003, www.klippel.de

## 10   APPENDIX

### 10.1   Two Signal Method

Substituting in Equation (18) the unknown parameter $S_S$ by the measured small signal transfer function $H_x(j\omega)$ between sound pressure p and displacement $x$ and using the estimated transfer function

$$H_F(j\omega) = k_0 + j\omega R_{MS} - \omega^2 m \qquad (23)$$

between displacement $x$ and force $F$ leads to the error equation

$$e = K(x) \cdot x + R_{MS}\frac{dx}{dt} + m\frac{d^2x}{dt^2} - L^{-1}\{H_x(j\omega)H_F(j\omega)\} * p \cdot \qquad (24)$$

Equation (24) may be significantly simplified by exciting the suspension with a sinusoidal tone at the resonance $\omega_R$ and writing the error signal in the frequency domain

$$e(t) = \sum_{i=0}^{N} E_i e^{ji\omega_R t} \qquad (25)$$

comprising the dc part $E_0$ and the complex amplitude $E_1$ of the fundamental at $\omega_r$ and the amplitudes $E_i$ of the ith-order harmonic at $\omega_{iR}=i\omega_R$ with $i > 1$.

For this special excitation signal we also consider the spectral components of the measured displacement

$$x(t) = \sum_{i=0}^{N} X_i e^{j\omega_{iR}t} \tag{26}$$

the calculated restoring force

$$F_K(t) = K(x)x = \sum_{i=0}^{N} F_i e^{j\omega_{iR}t} \tag{27}$$

and the measured sound pressure signal

$$p(t) = \sum_{i=0}^{N} P_i e^{j\omega_{iR}t} \ . \tag{28}$$

Combining Equation (24) with Equations (25)-(28) leads to the dc component

$$E_0 = F_0, \tag{29}$$

the fundamental component

$$E_1 = F_1 - m\omega_R^2 X_1 \tag{30}$$

and the $i$th-order harmonics (with i >1)

$$E_i = F_i + j\omega_{iR}R_{MS}X_i - m(\omega_{iR})^2 X_i \\ - H_x(j\omega_{iR})H_F(j\omega_{iR})P_i \ . \tag{31}$$

Under the condition that the mechanical resistance $R_{MS}$ is low compared with the imaginary part ($Q_{MS} > 2$) Equation (31) may be approximated by

$$E_i = F_i - \omega_R{}^2 m\left(i^2 X_i + \left(1 - i^2\right)H_x\left(j\omega_{iR}\right)P_i\right) \tag{32}$$

for $i > 1$.

The Equation (27) together with Equation (29), (30) and (32) are the basis for the estimation of the coefficients $k_i$ with $i \geq 0$.

## 10.2 One Signal Method

The identification of the nonlinear stiffness $K(x)$ may be simplified under the following conditions:

1.  The test enclosure has a relatively large volume (e.g. $V = 95$ Liter) giving a high acoustical compliance $C_{AB}$. This leads to the following relationship between the impedances

$$\left|\frac{S_s{}^2}{i\omega_0 C_{AB}}\right| << \left|S_s{}^2 Z_D\right| \tag{33}$$

for all $i$th-order harmonics ($i > 1$) generated by the distortion source $F_D$ in Fig. 8.

2.  If the diameter of the suspension part is also not very high or the porosity of the suspension material large giving a relatively low effective area $S_S$ then the compliance of the enclosed air transformed into the mechanical domain becomes much smaller than the stiffness of the suspension

$$\frac{S_s{}^2}{C_{ab}} << k_0 . \tag{34}$$

3.  If the losses of the mechanical resonator are relatively small ($Q_{MS} > 2$) then the impedance of the moving mass is much higher than the impedance of the losses

$$\omega_{iR} m > R_{MS} = \frac{\omega_0 m}{Q_{MS}} \tag{35}$$

for all $i$th-order harmonics ($i > 1$) generated by a sinusoidal excitation signal at resonance frequency $\omega_R$.

Under those conditions all harmonics generated by the distortion force $F_D$ in Fig. 8 fulfill the following relationship

$$F_D(x) + k_0 x + m \cdot \frac{d^2 x}{dt^2}$$
$$= K(x)x + m \cdot \frac{d^2 x}{dt^2} \approx 0 \tag{36}$$

because the low mechanical impedances of $C_{AB}$ is a shortcut in Fig. 8 for all harmonics in the total force $F$.

Also the fundamental component fulfills (36) at resonance frequency $\omega_R$. Only the total driving force corresponding to the sound pressure $p$

$$F = S_S p(t) \approx R_{MS} \frac{dx}{dt} \tag{37}$$

compensates for the mechanical losses and maintains the steady state vibration.

If the modeling uncertainties and numerical noise should be taken into account Equation (36) becomes

$$e = K(x) \cdot x + m \cdot \frac{d^2 x}{dt^2} \tag{38}$$

which is the basis for the parameter estimation.